

Journal Pre-proof

Rational Design for Controlled Release of Dicer-substrate SiRNA Harbored in phi29 pRNA-based Nanoparticles

Daniel W. Binzel, Songchuan Guo, Hongran Yin, Tae Jin Lee, Shujun Liu, Peixuan Guo

PII: S2162-2531(21)00189-X

DOI: <https://doi.org/10.1016/j.omtn.2021.07.021>

Reference: OMTN 1335

To appear in: *Molecular Therapy: Nucleic Acid*

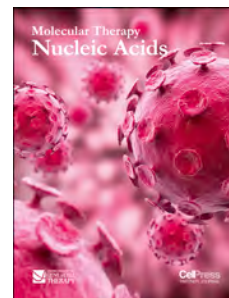
Received Date: 9 March 2021

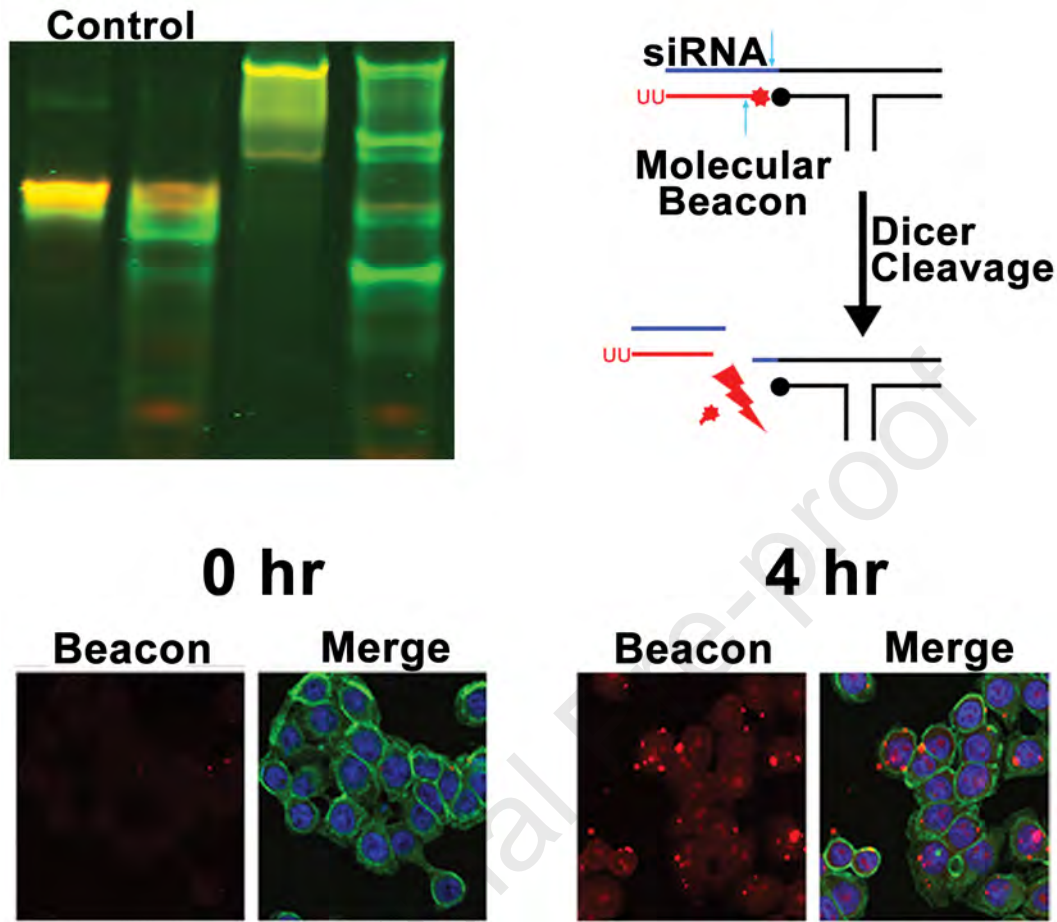
Accepted Date: 30 July 2021

Please cite this article as: Binzel DW, Guo S, Yin H, Lee TJ, Liu S, Guo P, Rational Design for Controlled Release of Dicer-substrate SiRNA Harbored in phi29 pRNA-based Nanoparticles, *Molecular Therapy: Nucleic Acid* (2021), doi: <https://doi.org/10.1016/j.omtn.2021.07.021>.

This is a PDF file of an article that has undergone enhancements after acceptance, such as the addition of a cover page and metadata, and formatting for readability, but it is not yet the definitive version of record. This version will undergo additional copyediting, typesetting and review before it is published in its final form, but we are providing this version to give early visibility of the article. Please note that, during the production process, errors may be discovered which could affect the content, and all legal disclaimers that apply to the journal pertain.

© 2021 The Author(s).





1 **Rational Design for Controlled Release of Dicer-substrate siRNA**
2 **Harbored in phi29 pRNA-based Nanoparticles**

3 Daniel W. Binzel^{1,#}, Songchuan Guo^{1,#,†}, Hongran Yin^{1,#}, Tae Jin Lee², Shujun Liu³, and Peixuan
4 Guo^{1,*}

5
6 ¹*Center for RNA Nanobiotechnology and Nanomedicine; Division of Pharmaceutics and*
7 *Pharmacology, College of Pharmacy; Dorothy M. Davis Heart and Lung Research Institute;*
8 *James Comprehensive Cancer Center; College of Medicine; The Ohio State University,*
9 *Columbus, Ohio 43210, USA.*

10 ²*Department of Neurosurgery, McGovern Medical School, The University of Texas Health*
11 *Science Center at Houston, Houston, Texas 77030, USA*

12 ³*The Hormel Institute, Masonic Cancer Center, University of Minnesota, Austin, Minnesota*
13 *55912, USA*

14 [#]*These authors contributed equally*

15
16 Short Title: Controlled Release of siRNA from RNA Nanoparticles

17
18 ***Correspondence should be addressed to:**

19 **Peixuan Guo, PhD**, Sylvan G. Frank Endowed Chair in Pharmaceutics and Drug Delivery, The
20 Ohio State University, 912 Biomedical Research Tower (BRT), 460 W. 12th Ave, Columbus,
21 Ohio 43210, USA. Email: guo.1091@osu.edu.

22 [†] **Current address:**

23 Department of Medicine, New York University Grossman School of Medicine

24

25 **Abstract**

26 SiRNA for silencing genes and treating disease has been a dream since ranking as a top
27 Breakthrough of the Year in 2002 by *Science*. With the recent FDA approval of four siRNA-
28 based drugs, the potential of RNA therapeutics to become the third milestone in pharmaceutical
29 drug development has become a reality. However, the field of RNAi therapeutics still faces
30 challenges such as specificity in targeting, intracellular processing, and endosome trapping after
31 targeted delivery. Dicer-substrate siRNAs included onto RNA nanoparticles may be able to
32 overcome these challenges. Here we show that pRNA-based nanoparticles can be designed to
33 efficiently harbor the Dicer-substrate siRNAs for *in vitro* and *in vivo* to the cytosol of tumor cells
34 and release the siRNA. The structure optimization and chemical modification for controlled
35 release of Dicer-substrate siRNAs in tumor cells were also evaluated through molecular beacon
36 analysis. Studies on the length requirement of the overhanging siRNA revealed that at least 23
37 nucleotides at the dweller's arm were needed for dicer processing. The above sequence
38 parameters and structure optimization were confirmed in recent studies demonstrating the release
39 of functional Survivin siRNA from the pRNA-based nanoparticles for cancer inhibition in non-
40 small-cell lung, breast, and prostate cancer animal models.

41 **Introduction**

42 RNA interference (RNAi) is a post-transcriptional gene regulation pathway used by different
43 classes of small RNAs.¹ Among them, small interfering RNAs (siRNA)² have attracted attention
44 for their important potentials in drug discovery and development. siRNA target and bind mRNA
45 to produce gene silencing effects, but their mechanisms are distinct.³ siRNA, for its ability to
46 silence genes and potential in treating diseases, has been a popular dream since *Science* ranked
47 this technology as a top ten Breakthrough of the Year in 2002.⁴ siRNA was first discovered in
48 1998 in *C. elegans* and in mammals in 2001.^{5, 6} Since many researchers have worked to bring
49 siRNA to the clinic until the recent FDA approval of Alnylam's Onpattro, the first siRNA drug.^{7,}
50 ⁸ Shortly thereafter the FDA has approved Givlaari and Oxlumo that were also developed and
51 produced by Alnylam.⁹⁻¹¹ Such FDA approvals have moved towards RNA becoming the third
52 milestone in pharmaceuticals, following chemical and protein based therapies.¹² However, the full
53 potential of siRNA into mainstream therapeutics has not been realized. Further strategies are
54 needed to avoid endosomal trapping.

55 siRNA is synthetically created, short RNA with matching sequence to its corresponding
56 mRNA. When internalized into cells, siRNA is incorporated into the RNA-induced silencing
57 complex (RISC), like microRNA.¹³ Classical siRNAs are short and typically only 19 bp in
58 length, although longer ones exist; alternatively, longer Dicer-substrate siRNAs range from 20-
59 27 bp and require Dicer processing.¹⁴ Both classical and Dicer-substrate siRNAs interact with
60 and activate RISC. The sense strand of siRNA is degraded,¹⁵ while the anti-sense strand
61 associated with RISC recognizes its target mRNA for cleavage by AGO2. However, the longer
62 Dicer-substrate siRNAs require Dicer processing before loading into RISC. It is reported that

63 Dicer-substrate RNA duplexes have increased gene silencing activity compared to classic 19-bp
64 siRNAs.¹⁶

65 For RNA to be considered for clinical applications it must be stable *in vivo*, thus demanding
66 stability against nucleases. In order to increase nuclease stability and reduce immunogenicity,
67 nucleotide sugar modifications can be used (most commonly 2'-Fluoro (2'-F), 2'-OMethyl, or
68 2'-O-methoxyethyl (2'-MOE)); however, Dicer-substrate siRNAs do not tolerate sugar
69 modifications at each position, since these modifications can interfere with Dicer recognition.
70 Therefore, careful consideration must be taken to increase siRNA stability. Researchers have
71 created nuclease stable siRNA while remaining sensitive to Dicer by only modifying key
72 nucleotide sites against nucleases and reducing off-target effects.¹⁷⁻²¹ 2'F, 2'-OMethyl
73 modifications on the sense strand and at the termini of anti-sense strands retained Dicer
74 processing. Additionally, 2'-MOE modifications were very site-specific due to the bulky size of
75 the modification. However, heavy modification of the anti-sense strand resulted in Dicer
76 inactivity. Understanding and exploiting Dicer processing is of significance in the design and
77 optimization of siRNA for efficient gene knockdown.

78 The Dicer enzyme belongs to the RNase III family, which can cleave long double-strand
79 RNAs into small RNAs.²² It is reported that the structure of the human Dicer is L shaped and
80 composed of a head, body and base.^{13, 22, 23} The head is the PAZ (piwi/ argonaute/ zwiller)
81 domain, which is also the RNA binding domain. PAZ domain has a high affinity for a 3'
82 protruding 2 nt overhang on RNAs. Two RNase III domains are located in the "body" and form
83 the processing center, where each RNAase III cleaves one of the long double-strand RNA. And
84 the base is an N-terminal DExD/H-box helicase domain with a clamp-shaped structure. Dicer can
85 cleave long ds-RNA into 21-22 bp ds-RNA. Dicer itself is like a molecular ruler since the

86 distance between the binding PAZ domain and cutting RNase III domain is about the length of
87 21-22 bp siRNA.^{24,25} Many factors affecting Dicer processing have been investigated, including
88 mutations to the PAZ domain responsible for RNA recognition, and in the design of siRNA in
89 relation to the 5'/3' structuring for Dicer binding and inclusion of chemical modifications
90 (discussed above).²⁶⁻²⁹ However, some conclusions are inconsistent or contradictory and seem to
91 be specific to each siRNA sequence.

92 To achieve *in vivo* gene knockdown, another key is efficient delivery of RNAi into cancer
93 cells. Although many nanocarriers have been developed, our studies^{12, 30, 31} have shown that
94 RNA nanotechnology provides one of the best strategies to deliver RNAi into cancer cells.³²⁻³⁴
95 By definition, RNA nanotechnology is the bottom-up construction of nanostructures composed
96 primarily of RNA, including the core scaffolding and any functional group attached to the
97 nanoparticle.³⁴ Since its conception, more and more complex RNA nanoparticles have been
98 constructed with high thermodynamic stability and proven to function well in *in vivo*
99 applications.^{32, 35-38} Our RNA nanoparticles, using the phi29 DNA packaging motor pRNA as a
100 core motif, are homogeneous in size, structure, and stoichiometry; are thermodynamically and
101 chemically (after 2'-F modifications) stable;^{36, 39-42} retain authentic folding and independent
102 functionalities of all incorporated modules (RNA aptamer, siRNA, miRNA or ribozyme);^{36, 43} are
103 non-toxic,^{42, 44} highly soluble, and display favorable biodistribution and PK/PD profiles.^{36, 39, 42,}
104 ⁴⁴⁻⁴⁶ Furthermore, the application of RNA nanoparticles to exosomes, 30-150 nm membranous
105 vesicles of endocytic origin as a way of intercellular communications,^{47, 48} allows for both the
106 loading of RNA nanoparticle-siRNA cargos and displaying tumor targeting ligands.³⁰ Exosomes
107 have an endomembrane-like membrane property (structure, lipid, peptides, protein, etc.) and
108 have been shown to carry genetic materials, especially RNA, as a form of intercellular

109 communication.⁴⁷⁻⁵⁴ Exosomes have been considered for their therapeutic applications due to
110 their favorable size and are well-tolerated *in vivo*.⁵¹ Therapeutic payloads, such as siRNA, can
111 remain fully functional after delivery to cells by exosomes.^{47, 48, 52, 55} These exosomes have
112 demonstrated their ability to fuse to the cell membrane of the targeted cells resulting in the
113 dumping of their cargo directly into the cytosol of cells.⁵⁶ As such we utilize these exosomes for
114 their ability to avoid endosome trapping and therefore increase the efficiency of delivered
115 siRNAs.⁵⁶

116 RNA nanotechnology has gained significant interest in the development of novel nano-
117 structures.⁵⁷⁻⁶⁴ Several researchers have used these RNA nanoparticles for the inclusion of RNAi
118 components, including siRNAs, and examined their specific gene silencing abilities.⁶⁵⁻⁷⁰ Similar
119 to our approaches of applying RNA nanoparticles to exosomes, complex delivery vehicles have
120 been created by functionalizing RNA nanoparticles with polymer nanoparticles⁷¹ and exosomes⁷²
121 for improved siRNA delivery. Thus RNA nanoparticles are poised to overcome the previous
122 roadblocks in siRNA therapies. However, little is known on how the delivered siRNA by RNA
123 nanoparticles and exosomes interacts with the Dicer complex to achieve efficient knockdown of
124 target genes.

125 In the present study we examine if Dicer-substrate siRNA can be incorporated onto pRNA
126 based RNA nanoparticles and their required design parameters to retain Dicer processing. We
127 integrate and test factors affecting Dicer processing, which directed us to design siRNA loaded
128 RNA nanoparticles that can function as a Dicer substrate to generate a robust gene regulation
129 tool. Dicer-substrate siRNA is used in these studies due to the ease of inclusion into RNA
130 nanoparticles by simple helical extension, increased efficacy in gene knockdown over short
131 siRNA, and reduced immune responses over short siRNA.^{14, 16} Unlike shorter siRNA, Dicer-

132 substrate siRNA has not translated to the clinic due to delivery issues and requirements of Dicer
133 processing, here we aim to overcome these issues. Besides inclusion of 3'- two nucleotides
134 overhangs and a 5'-phosphate group, we also investigated whether chemical modifications affect
135 Dicer processing. Based on the screened factors, Luciferase 2 (*LUC2*) siRNA was designed to be
136 incorporated into RNA nanoparticles. To demonstrate the Dicer processing, a molecular beacon
137 was designed and constructed to monitor the activity. Our findings suggest that an integration of
138 length, nucleotide components, structure, and RNA nanotechnology into the designs of RNAi
139 achieves efficient silencing of targeted genes in an *in vivo* cancer therapy setting. As such our
140 findings provide design parameters for siRNA incorporation into RNA nanoparticles for efficient
141 gene silencing.

142

143 **Results**

144 ***RNA nanoparticles harboring siRNA were processed by Dicer into functional*** 145 ***siRNA resulting in cleavage of target gene***

146 RNA nanoparticles based on the phi29 pRNA were constructed to include Lamin25 siRNA
147 extended on the pRNA 5'/3' terminal end (pRNA-Lamin25). Lamin A/C was chosen as a model
148 gene to demonstrate the specific cleavage of mRNA by a 5' RACE (rapid amplification of cDNA
149 ends) technique to prove that the gene silencing activity of pRNA nanoparticle is mediated by
150 RNA interference.⁷³ pRNA-Lamin25 was designed similar to that described by Zhang *et al*,⁷⁴
151 with 25 bp siRNA linked to a pRNA vector by a double uracil (-UU-) linker (**Fig. 1A**). RNA was
152 prepared by *in vitro* transcription by T7 RNA polymerase and transfected into KB cells. The
153 gene silencing efficiency of pRNA-Lamin25 was first demonstrated by quantitative qRT-PCR
154 (**Fig. S1**). A RNA ligation step and two rounds of PCR was used to reveal the sequence of

155 mRNA after cleavage. A DNA fragment representing the cleaved mRNA was detected in the
156 pRNA-Lamin25 sample with the size between 200 bp and 300 bp in gel electrophoresis (**Fig.**
157 **1B**). The mRNA cleavage was expected to be 243 bp in length indicating successfully cleaved
158 Lamin A/C. Sequencing results of the excised DNA fragment confirmed that Lamin A/C mRNA
159 was cleaved at a position ten nucleotide from the 5' end of the antisense of Lamin25 siRNA
160 sequence as predicted. No fragment was detected in the control samples treated with pRNAi-
161 scramble (**Fig. 1B-lane 2**). These data demonstrate that gene silencing mediated by the pRNA-
162 siRNA is induced by RNAi pathway as in standard siRNA duplex. The incorporation of siRNA
163 into RISC and cleaving the Lamin A/C mRNA proves RNA nanoparticles are able to deliver
164 siRNA sequences into cancer cells and specifically silence its respective gene.

165

166 *Development of RNA nanoparticle molecular beacons for observation of in vitro* 167 *processing and release of siRNA*

168 Based on the above results, it was determined that siRNA sequences can release from RNA
169 nanoparticles within the cells. However, confirmation of Dicer processing of siRNA from RNA
170 nanoparticles has not been observed, nor is it understood the release mechanism of siRNA from
171 the RNA nanoparticles. pRNA-3WJ RNA nanoparticles were constructed incorporating 24 bp,
172 3'-UU overhang luciferase siRNA oligo (*LUC2*-siRNA). The pRNA-3WJ motif was used in
173 these studies due to ease of construction and the multivalent nature of the pRNA-3WJ allows for
174 inclusion of siRNA on one helical branch while targeting ligands, such as RNA aptamers, can be
175 added to other branches to fulfill specific and favorable cancer targeting.^{36, 44, 45, 75} This design
176 takes advantage of the high chemical and thermodynamic stability as well as multivalency of the
177 3WJ scaffold for therapeutics loading and delivery.^{38, 76} To demonstrate that the siRNA

178 incorporated to 3WJ RNA nanoparticles could be processed by Dicer for higher gene regulation
179 efficacy, a molecular beacon was designed accordingly by introducing a fluorophore/quencher
180 pair into the nanoparticles (**Fig. 2A**). A Cy5 fluorophore was conjugated to 5'-end of antisense
181 strand while a BBQ650 fluorescence quencher was attached to 3'-end of 3WJ-c strand adjacent
182 to the Cy5 label. Such design quenches the Cy5-siRNA signal until the siRNA is processed by
183 Dicer, thus creating a short, Cy5-labeled sequence on the 3WJ nanoparticle that is quickly
184 dissociated due to lack of strong base pairing resulting in recovery in fluorescent signal.

185 Stepwise assembly of the 3WJ/*LUC2*-siRNA was confirmed by 15% polyacrylamide gel in
186 native folding conditions, and incorporation of BBQ650 resulted in high quenching of the Cy5
187 signal (**Fig. 2B**). Serum stability and Temperature Gradient Gel Electrophoresis (TGGE) studies
188 proved resulting nanoparticles that have high chemical and thermodynamic stability, respectively
189 (**Fig. 2C** and **2D**), which guarantees the low background noise signal due to lack of *in vivo*
190 degradation of the nanoparticles.

191 This 3WJ-*LUC2*-siRNA beacon design was used to monitor Dicer processing by intracellular
192 imaging. When the nanoparticle is intact, Cy5 signal is quenched by the BBQ650 due its close
193 proximity and low fluorescence could be detected (“OFF” status). The Cy5 fluorescence is
194 restored when the nanoparticles underwent processing by Dicer and the short fragment with Cy5
195 fell off of the nanoparticle creating distance with the BBQ650 (“On” status) (see **Fig. 2A**). By
196 comparing the fluorescence intensities between 3WJ/*LUC2*-siRNA-Cy5 and 3WJ/*LUC2*-siRNA-
197 Cy5/BBQ650 (molecular beacon), we have a better understanding about the processing of the
198 siRNA in the cell cytosol and its processing efficiency.

199

200 ***Direct observation of in vitro siRNA processing from RNA nanoparticles***

201 Exosomes are lipid vesicles released from cells typically for intercellular communications.⁷⁷
202 We previously modified the isolated exosomes from HEK293 cells with RNA nanoparticles, and
203 demonstrated that RNA displaying exosomes are able to deliver loaded cargos directly to the
204 cytosol of cells.^{30, 56, 78} HEK293 exosomes were previously shown to have an average size of 96
205 nm via Nanoparticle Tracking Analysis, a negative zeta potential of -4.6 mV via Dynamic Light
206 Scattering, and expression of TSG101, a typical exosome specific marker.⁷⁹ With concerns of
207 cytosol trapping, thus preventing siRNA from releasing into the cytosol, we loaded 3WJ/*LUC2*-
208 siRNA beacon nanoparticles into exosomes to be delivered to HT29 cells with continuous
209 luciferase expression (HT29-luc). Additionally, the exosomes were decorated with previously
210 developed RNA nanoparticles harboring folate to provide specific targeting and binding to the
211 folate receptor expressing HT29 cells.³⁰ Confocal fluorescent microscopy and flow cytometry
212 (FACS) demonstrated high binding efficiency of folate targeting exosomes (FA/EV/*LUC2*-
213 siRNA/Cy5) to the HT29-luc cells (**Figure S2A**) and internalization of the 3WJ/*LUC2*-
214 siRNA/Cy5 loaded into the exosomes over controls (**Fig. S2B**). A clear shift in peak
215 fluorescence of the HT29 cells was seen in both FACS and confocal studies of the
216 FA/EV/*LUC2*-siRNA/Cy5 over the 3WJ/EV/*LUC2*-siRNA/cy5 with nearly triple the
217 fluorescence intensity seen in the FACS results.

218 Utilizing the exosome delivery vehicle allowed the 3WJ/*LUC2*-siRNA beacon nanoparticles
219 to be efficiently distributed to the cytosol of the cancer cells for a time-course study of siRNA
220 processing by Dicer. As a positive control to demonstrate Dicer processing rather than random
221 RNase degradation, a truncated 19 bp *LUC2*-siRNA was placed onto the 3WJ (S1: 3WJ/*LUC2*-
222 siRNA-tru) (**Fig. 3A**). 3WJ/*LUC2*-siRNA/Cy5 (S3) nanoparticles were also tested as a total Cy5
223 signal control. 3WJ/*LUC2*-siRNA beacon (S2) as well as control nanoparticles were delivered by

224 the folate displaying exosomes. The processing of siRNA from 3WJ scaffold was reflected by
225 Cy5 fluorescence gradual increase in signal over time, as shown in confocal microscopy studies
226 (**Fig. 3B-3D**). As such the data directly demonstrated that Dicer is able to bind and cleave siRNA
227 incorporated into RNA nanoparticles. This proved that the RNA nanoparticle motif does not
228 interfere with Dicer siRNA processing due to steric hindrance or processing issues as a result of
229 the nanoparticles' branched nature. It is noted that fluorescence in the 3WJ/*LUC2*-siRNA/Cy5
230 positive control, fluorescence intensity increases over time due to the longer incubation time of
231 the RNA nanoparticle/exosome complex with cells. This allows for increased levels of
232 3WJ/*LUC2*-siRNA/Cy5 to be released in the cells resulting in higher fluorescence levels over
233 time. However, such control serves as a siRNA delivery vehicle control to ensure that siRNA is
234 being delivered within cells.

235

236 ***In vitro identification of the specific cleavage site of siRNA by Dicer as RNA*** 237 ***nanoparticle design principle***

238 In order to better understand the Dicer processing of siRNA from our RNA nanoparticles and
239 provide design principles for siRNA incorporation onto RNA nanoparticles, we examined Dicer
240 processing to various siRNAs *in vitro*. Rational design of siRNA should be illustrated when
241 considering incorporation to RNA nanoparticles to ensure the intracellular Dicer processing of
242 siRNA. Therefore, different factors affecting Dicer processing including siRNA length, 5'-
243 phosphate, 3'-two nucleotides overhang, and 2'-F modifications were tested based on the
244 Luciferase2-siRNA used above. The base pairing length is a key factor as Dicer processes
245 siRNA according to the loop-counting rule.⁸⁰ DsRNA substrate is anchored to the PAZ domain
246 and the specified distance between the anchored helical end of the dsRNA and the RNase active

247 site in the RNaseIII domains serves as a molecular ruler.^{2, 27, 81} To test the cleavage based on the
248 loop-counting rule, different lengths (19 bp, 21 bp, 22 bp, 23 bp and 24 bp) of *LUC2*-siRNAs
249 were designed and constructed (**Table S1**) to be tested for Dicer processing using Human
250 Recombinant Dicer Enzyme. After incubation with the Dicer enzyme, 3WJ-siRNA conjugates
251 were assayed by polyacrylamide gel looking for a cleaved product. The results demonstrated that
252 siRNA longer than 21 bp showed obvious processing, and 24 bp *LUC2*-siRNA could be
253 processed with the highest efficiency (**Fig. 4A**). Shortening either strand of the double-stranded
254 *LUC2*-siRNAs resulted in inhibition of Dicer processing (**Fig. 4B**), which is due to the dimer
255 structure of RNaseIII domain. In addition, siRNA constructs regarding 5'-phosphate, 3'-UU
256 overhang and 2'-F modification were tested for Dicer processing (**Fig. 4C**). 2'-F modifications
257 were selected as they are well studied in our pRNA-3WJ system and have shown not to affect the
258 3WJ structuring while increasing thermodynamic and enzymatic stabilities.^{38, 76} Quantification of
259 Dicer processed bands demonstrated that the absence of 3'-UU reduces Dicer processing
260 efficiency to only 62% (**Fig. 4C lane 5**), which may be due to less favorable Dicer enzyme
261 binding. When including enzyme stabilizing chemical modifications, 2'-F modifications to the
262 pyrimidines of the siRNA sense strand also decreased the processing to 45% (**Fig. 4C lane 3**);
263 however, the presence of a 5'-phosphate to the sense strand did not affect Dicer processing much
264 in our testing (**Fig. 4C lane 2&4**). While the decreased Dicer processing in adding 2'-F
265 modifications is disappointing, these modifications are typically required for *in vivo* applications
266 for the increased thermodynamic and enzymatic stabilities of the RNA nanoparticles. However,
267 the incorporation of the 3'-UU overhang of the anti-sense strand significantly improves Dicer
268 processing.

269 From our testing we were able to further demonstrate loading of siRNA onto RNA
270 nanoparticles still allows for Dicer recognition and processing of the siRNA (**Fig. 4D**). The use
271 of the molecular beacon demonstrated that 24 bp siRNA is cleaved from the nanoparticle
272 resulting in Cy5 signal. Dicer processing of various siRNA designs indicated that when
273 incorporating siRNA onto RNA nanoparticles, the length of the siRNA must remain at a
274 minimum length of 22 bp.

275

276 ***Functional siRNA releasing from the RNA nanoparticles has been confirmed in***
277 ***multiple animal trials on lung, breast, and prostate cancer models.***

278 Furthermore, our group has proven the *in vivo* delivery of siRNA via RNA nanoparticles
279 harboring Survivin siRNA loaded into exosomes (**Fig. 5**).^{30, 82} Microscopy studies demonstrated
280 that the exosomes allow for membrane fusion and cytosol dumping of therapeutic cargos,⁵⁶ while
281 resulting in ultra-high inhibition of tumor growth in *in vivo* tumor models.³⁰ While it is thought
282 that endosome entrapment can allow for the slow release of stable siRNA into the cells,⁸³ our
283 exosomes avoid endosome entrapment and create direct siRNA delivery to the cytosol of
284 targeted cells for swift treatment.⁵⁶

285 The releasing of functional siRNA from our RNA nanoparticles was documented by animal
286 trials in multiple publications showing the inhibition of tumors in non-small-cell lung
287 (NSCLC),⁸² triple negative breast (TNBC),³⁰ and prostate cancer³⁰ models when Survivin siRNA
288 was fused onto RNA nanoparticles and delivered to tumors (**Fig. 5**). Prostate specific membrane
289 antigen (PSMA) RNA aptamers allowed for specific targeting and delivery of the siRNA to
290 PSMA+ prostate xenograft tumors in nude mice using LNCaP-LN3 cells.³⁰ Additionally,
291 epidermal growth factor (EGFR) RNA aptamers were displayed on the surface of exosomes for

292 delivery to orthotopically developed TNBC tumors using MDA-MB-468 cells³⁰ and separately
293 NSCLC xenograft tumors using H596 cells.⁸² Exosomes were delivered intravenously via tail-
294 vein injection. **Figure 5** demonstrated that, across three tumor models, exosomes modified with
295 RNA nanoparticles are able to deliver Survivin siRNA that is then processed in the tumors
296 resulting in strong tumor inhibition. Full data on these studies can be found in Pi, *et al. Nat*
297 *Nanotechnol*, 2018; 13(1):82-89 and Li *et al. Nucleic Acid Ther* 2021; ahead of print.^{30, 82}

298

299 **Discussion**

300 Since its discovery in 1999,⁵ siRNAs and other RNAi sequences have shown great promise
301 in treating diseases and cancers by silencing specific responsible genes. Many large
302 pharmaceutical companies and research groups have invested billions of dollars towards
303 developing siRNA and other RNAi technologies for the treatment of cancers.⁸⁴⁻⁸⁸ However,
304 difficulties in producing a safe and efficient delivery system for the siRNA resulted in
305 diminishing interest. Yet the promise of siRNA for the treatment of cancers and viral-infections
306 still remains.⁸⁹ There is a desperate need for more efficient delivery vehicles that not only
307 specifically target disease sites with high affinity but also deliver the RNAi payloads for Dicer
308 processing.

309 In the presented study, the pRNA based RNA nanoparticles resulted in the specific
310 knockdown and gene silencing via siRNA delivery. Our cell microscopy studies involving
311 siRNA beacons conjugated to RNA nanoparticles demonstrate a time release study of siRNA
312 from the RNA nanoparticles by Dicer processing. As a result of the siRNA release and
313 incorporation into RISC, target Lamin A/C mRNA was cleaved as demonstrated in **Fig. 1**. These
314 experiments prove that the RNA nanoparticles do not inhibit or limit the Dicer binding, reading,

315 or processing of siRNA due to their three-dimensional shapes. Additionally, in understanding
316 Dicer processing of siRNA, several design principles of siRNA incorporation into RNA
317 nanoparticles were created. First, the length of incorporated siRNA is very important, in that a
318 minimum 22 nt sequence of the anti-sense strand is needed, with 24 nt showing the best
319 processing efficiency by Dicer. Additionally, we have demonstrated that 2'-F modifications to
320 the siRNA sense strand and removal of the 3'-UU overhang of the siRNA anti-sense results in
321 reduced Dicer processing, but still produces siRNA product for gene knockdown. The reduced
322 Dicer processing of the 2'-F modified siRNA is similar to that seen in studies by other groups
323 looking at using 2'-F and 2'-OMethyl modifications on siRNA without nanoparticles.^{90, 91}
324 Collingwood *et al.* completed various modifications to both sense and anti-sense strands and
325 overall reported reduced activities for Dicer processing.⁹⁰ However, some modifications to
326 siRNA have demonstrated an increased potency and even the ability to incorporate into RISC
327 without being processed by Dicer.^{91, 92} As a whole, these studies advance our understanding of
328 the role of RNA nanoparticle design to maximize the efficiency of siRNA delivery to cancer
329 tumor cells. Additionally, these design parameters ensure RNA nanoparticles to be stable and are
330 able to reach tumors *in vivo*. Moving forward these studies will be implemented.

331 RNA nanoparticles provide a stable *in vivo* delivery platform of RNAi, where target tissue
332 specificity can be enhanced via conjugation of tumor-targeting ligands in addition to their
333 rubber-like properties.^{33, 93} Currently there are three platforms for delivery of siRNAs in clinical
334 trials or approved by the FDA.⁹⁴ These include lipid-based nanoparticles (LNPs),⁹⁵⁻⁹⁷ *N*-
335 acetylgalactosamine conjugated siRNA (GalNac-siRNA),⁹⁸⁻¹⁰⁰ and targeted RNAi Molecule
336 (TRiM).^{101, 102} These siRNA delivery platforms have become increasingly efficient at delivering
337 siRNAs by now including targeting ligands. However, many of them typically accumulate in

338 liver and lungs. However, RNA nanoparticles have demonstrated their ability to avoid strong
339 accumulation in the liver, lungs, and other healthy organs with only having strong accumulation
340 in targeted tumors. Also, unlike other GalNAC-siRNA conjugates that only target hepatocytes,
341 RNA nanoparticles are able to harbor a variety of targeting ligands to target and accumulate in a
342 variety of cancers including colon, breast, prostate, gastric, liver and glioblastoma.^{45, 46, 75, 103-105}
343 The rubbery property, ability to deform shape under force and return to its original form upon
344 relaxation, of RNA nanoparticles allows for a strong passive targeting effect to cancers, while
345 being able to slip through glomerular filtration and excrete to urine through the kidneys before
346 creating toxicity to healthy organs.⁹³

347 Additionally, RNA nanoparticles have been used to deliver dicer-substrate siRNAs to tumor
348 sites resulting in specific gene silencing and tumor inhibition. Cui *et al.* delivered *BRCA1*
349 siRNA to gastric cancer tumors in mice using the pRNA-3WJ labeled with folic acid.⁴⁴ The
350 folate conjugated onto the nanoparticle allowed for specific binding and internalization to gastric
351 cancer cells while specifically silencing *BRCA1* leading to tumor growth inhibition. In a similar
352 fashion, Lee *et al.* delivered luciferase siRNA as a proof of concept to glioblastoma tumors using
353 folic acid targeting to the overexpression of folate receptors on the tumor model.⁴⁶ Additionally,
354 Zhang *et al.* utilized the pRNA-3WJ platform to deliver *MED1* siRNA to breast cancer tumors in
355 mice to overcome tamoxifen resistance.¹⁰⁶ The silencing of *MED1* by the RNA nanoparticles led
356 to tumor inhibition as well as resensitization to tamoxifen, thus decreasing lung metastasis and
357 cancer stem cell content. Xu *et al.* demonstrated the silencing of Delta-5-Desaturase (*D5D*) by
358 pRNA-3WJ nanoparticles alongside the DLGA treatment for the colon cancer suppression.¹⁰⁷
359 Here our studies build upon this foundation of using RNA nanoparticles to deliver siRNA to
360 cancers by examining the design properties of the substrate siRNA. Past studies have focused on

361 incorporating 19 nt anti-sense siRNA onto 3WJ RNA nanoparticles; however, here we proved
362 that longer 24 nt siRNA provides an increase in Dicer processing. Additionally, careful
363 consideration must be taken for the chemical modification of the siRNA sense strand. The
364 proven ability of RNA nanoparticles to deliver RNAi components specifically to tumors further
365 aids in moving RNA as the third milestone in pharmaceuticals following small molecule and
366 protein based drugs.

367

368 **Materials and methods**

369 *Preparation of RNA nanoparticles harboring siRNAs*

370 pRNA-lamin25 nanoparticles were designed with the lamin targeting siRNA extended off the
371 3'/5' proximate end of the phi29 pRNA. The sequence of the single stranded RNA nanoparticle
372 is shown in **Figure S3**. Nanoparticles were constructed via bottom-up assembly through the
373 construction of a dsDNA template including the T7 RNA polymerase promoter. RNA was
374 transcribed *in vitro* by T7 RNA polymerase using previously described procedures in the Guo
375 lab.^{40, 108}

376 Different DS/*LUC2*-siRNAs were designed to study factors affecting Dicer processing.
377 3WJ/*LUC2*-siRNA molecular beacon was designed to study intracellular Dicer processing. The
378 sequences are listed in **Table S1** and **Table S2**. Each short oligo strand to compose the 3WJs was
379 prepared by solid phase synthesis using an oligo-synthesizer as described previously.¹⁰³
380 Molecular beacon was added to the 3WJ nanoparticles by attaching a Cy5 fluorophore to 5'-
381 *LUC2*-antisense strand using Cy5-Phosphoramidite while BBQ650 was conjugated to 3'-3WJ-c
382 using BBQ650-CPG column. All strands were synthesized, desalted and purified before use.

383 To assemble into DS- or 3WJ- nanoparticles, equal molar ratios of each component strand
384 was mixed together in 1× TMS buffer (50 mM Tris (pH 7.6), 100 mM NaCl, 10 mM MgCl₂),
385 heated to 90 °C for 5 min and slowly cooled to 37 °C on a thermocycler.

386

387 *Cell culture*

388 KB cells were cultured in RPMI-1640 medium (Life Technologies) containing 10% FBS in a
389 37 °C incubator under 5% CO₂ and a humidified atmosphere. HT29 cells were cultured in
390 RPMI-1640-Folate deficient medium (Life Technologies) containing 10% FBS in a 37 °C
391 incubator under 5% CO₂ and a humidified atmosphere.

392

393 *Detection of lamin A/C siRNA knockdown by 5' RACE*

394 100 nM pRNA-lamin25 was transfected into KB cells using FuGENE HD (Roche,
395 Indianapolis). Cells were harvested 48 hr after transfection. Total mRNA was isolated using
396 Poly(A)Purist™ Kit (Ambion, Austin). FirstChoice® RLM-RACE Kit (Ambion, Austin) was
397 used in the 5' RACE experiment or known as single-sided PCR. Using primers for the middle of
398 the unknown sequence, mRNA is amplified in the full length therefore amplifying either the
399 cleaved and shortened mRNA from the siRNA or amplifying the much longer uncleaved mRNA.
400 Thus, the PCR amplification allows for easy differentiation of cleaved product. The sequences of
401 primers used in this study are:

402 Lamin Gene specific 3' primer: 5'-CCAGTGAGTCCTCCAGGTCTCGAAG-3'

403 Lamin Gene specific 3' nested primer: 5' CCTGGCATTGTCCAGCTTGGCAGA-3'

404

405 *In vitro siRNA processing using Recombinant Human Dicer enzyme*

406 To examine the Dicer processing, 1 μ g of RNA nanoparticles were incubated with 2 μ l
407 Recombinant Human Dicer Enzyme (Genlantis) following manufacture's instruction. After 6 hr
408 incubation at 37 °C, 20% Native PAGE was used to check the product before and after the Dicer
409 processing. The gel was run in TBM buffer at 150 V for 1.5 hr, stained with Ethidium bromide
410 (EB) and imaged on a Typhoon FLA7000 (GE) for EB and Cy5 signal.

411

412 *Stability studies of 3WJ/LUC2-siRNA nanoparticles*

413 The serum and thermodynamic stability of 3WJ/LUC2-siRNA were studied using the
414 procedures previously described.^{38, 76} In short RNA nanoparticles were incubated in 10% fetal
415 bovine serum for 0-24 hr and ran on 15% TBM polyacrylamide gel electrophoresis (PAGE). Gel
416 bands were quantified by ImageJ and plotted as Stable RNA/Total RNA. Thermodynamic
417 stability was examined by running RNA nanoparticle in temperature gradient gel electrophoresis
418 (TGGE) with a temperature gradient (20-80 °C) perpendicular to the electrophoretic current.
419 Bands were quantified by ImageJ and plotted in a similar fashion. 15% TBM PAGE was run to
420 check the integrity and purity of the nanoparticles.

421

422 *Purification of exosomes*

423 Exosomes were purified using a modified differential ultracentrifugation method as
424 previously described.^{30, 56, 78} HEK293T cells obtained from ATCC were cultured in FiberCell
425 Hollow Fiber Bioreactor (C2011, 20kDa MWCO) using DMEM medium with 10% exosome
426 free FBS. Exosome-enriched media were collected every week from the bioreactor. Exosome
427 enriched media were spun down at 300 rcf for 10 min to remove cells, followed by spinning at

428 10,000 rcf for 30 min at 4 °C followed by 22 nm filtration to remove cell debris and micro
429 vesicles and store at -80 °C until 500 mL accumulated.

430 Pre-processed media were thawed slowly at 4°C overnight, then loaded into a pre-
431 conditioned Pall Minimate™ TFF system with 100kDa MWCO capsule (OA100C12),
432 precondition following standard operation by manufacture. 500 mL exosomes-enriched media
433 were processed at 6 mL/min by setting pump speed at 40 mL/min. When volume reduced to ~ 5
434 mL, 200 mL sterile DPBS was added as a washing step and continued to run until the volume
435 reduced to ~ 5 mL again, then collected. Two 15 mL DPBS wash steps were performed and total
436 30 mL wash was collected and combined with the 5 mL sample from last step.

437 The 35 mL post TFF media were then further purified by 100,000 rcf ultracentrifugation
438 using a SW28 rotor (Beckman Coulter) for 90 min at 4 °C. 200 µl of 60% iodixanol (Sigma) was
439 added to the bottom of each tube to serve as iso-osmotic cushion as previously reported.^{30, 56, 78}
440 The supernatant was carefully removed from the top and around 2 ml of the fraction close to the
441 interface and cushion was collected.

442

443 *Exosome characterization*

444 Nanoparticle Tracking Analysis (NTA) was carried out using the Malvern NanoSight NS300
445 system on exosomes re-suspended in PBS at a concentration of 10 µg of protein per millilitre for
446 analysis following published methods.⁷⁹ Three 10-second videos recorded all events for further
447 analysis by NTA software. The Brownian motion of each particle is tracked between frames,
448 ultimately allowing for calculation of the size through application of the Stokes–Einstein
449 equation.

450 Purified exosomes were assayed for exosomal protein markers via Western blot. Exosomes
451 were loaded onto TDX FastCast SDS PAGE gels (BioRad, Hercules, CA), ran at 100 V for 2
452 hours, and transferred from gel to membrane. Membranes were blocked by 5% fat-free milk at
453 room temperature for 1 h and incubated overnight in primary antibody. Protein bands were
454 detected with an ECL system (Pierce) after incubating in the HRP-conjugated secondary
455 antibody for 1 h at room temperature and exposed to film for autoradiography. Primary
456 antibodies used for western blot analysis were rabbit anti-human *TSG101* (Thermo Scientific,
457 PA5-31260), rabbit anti-human integrin $\alpha 4$ (Cell Signaling, 4711S), rabbit anti-human integrin
458 $\alpha 6$ (Cell Signaling, 3750S), rabbit anti-human integrin $\beta 1$ (Cell Signaling, 4706S), rabbit anti-
459 human integrin $\beta 4$ (Cell Signaling, 4707S), rabbit anti-human integrin $\beta 5$ (Cell Signaling,
460 4708S), rabbit anti-human Glypican 1 (Thermo Fisher, PA5-28055).

461

462 *Loading of 3WJ/LUC2-siRNA and 3WJ/siSur into FA/EV and EGFR/EV*

463 Exosomes (EV) (100 μ g of total protein) and RNA nanoparticles harboring *LUC2* siRNA or
464 Survivin siRNA (10 μ g) were mixed in 100 μ l of PBS with 10 μ l of ExoFect Exosome
465 transfection (System Biosciences), followed by a heat-shock protocol to complete the RNA
466 nanoparticle loading. Cholesterol-modified 3WJ/FA or cholesterol-modified 3WJ/EGFR (or
467 3WJ) nanoparticles were incubated with RNA-loaded exosomes for decoration at an average
468 ratio of 5000:1 (RNA:exosome) at 37 °C for 45 min, then left on ice for 1 hr to prepare the
469 FA/EV and EGFR/EV. To purify RNA-decorated EVs, 400 μ l of RNA-decorated EVs were
470 washed with 5 ml PBS in a SW-55 tube that contained 20 μ l of 60% iodixanol cushion and spun
471 at 100,000 g for 70 min at 4 °C. All the pellets in the cushion were collected and suspended in
472 400 μ l of sterile PBS for further use.

473

474 *Binding and internalization assay of FA/Exo/Luc2-siRNA*

475 For cell binding assays, HT29 cells were incubated with FA/EV/*LUC2*-siRNA/Cy5,
476 3WJ/EV/*LUC2*-siRNA/Cy5, 3WJ/FA/*LUC2*-siRNA/Cy5, 3WJ/*LUC2*-siRNA/Cy5 at 37 °C for 1
477 hr before Flow Cytometry. Samples were incubated at a concentration of 100 nM of the Cy5
478 RNA strand.

479 To study internalization, FA/EV/*LUC2*-siRNA/Cy5 as well as control groups including
480 3WJ/EV/*LUC2*-siRNA/Cy5, EV/*LUC2*-siRNA/Cy5 were incubated with HT29 cells at 37 °C for
481 1 hr. Samples were incubated at a concentration of 100 nM of the Cy5 RNA strand. After
482 washing with PBS, the cells were fixed by 4% paraformaldehyde and stained by Alexa Fluor®
483 488 phalloidin (Invitrogen) following manufacturer's instructions and DAPI for cell nucleus
484 staining and mounted with ProLong[®] Gold Antifade Reagent (Life Technologies Corp.,
485 Carlsbad, CA). The cells were then analyzed for binding and cell entry by an Olympus FV3000
486 Confocal System microscope.

487

488 *Intracellular imaging of siRNA processing from 3WJ via molecular beacon*

489 To monitor intracellular Dicer processing, RNA nanoparticles (3WJ/*LUC2*-siRNA-tru
490 beacon, 3WJ/*LUC2*-siRNA beacon, 3WJ/*LUC2*-siRNA Cy5) were loaded to exosomes
491 respectively, further decorated by FA as described above. After incubation with HT29 cells for
492 0.5, 2 and 4 hr, cells were fixed and stained as described above. Samples were incubated at a
493 concentration of 100 nM of the Cy5 RNA strand. Cy5 signal was monitored for each group at
494 different time point by confocal microscopy under the same parameters.

495

496 **Conclusions**

497 Through the completed studies we aimed to demonstrate the efficient processing of siRNA
498 from RNA nanoparticles for high gene silencing, while providing a comprehensive, mechanistic
499 understanding of siRNA Dicer processing from RNA nanoparticles. As such, our pRNA-
500 Lamin25 and 3WJ-*LUC2* beacon nanoparticles proved intercellular Dicer cleavage, RISC
501 incorporation, and specific mRNA cleavage. Furthermore, our in-depth studies of Dicer
502 processing of siRNA and RNA nanoparticle/siRNA conjugates proved not only that the RNA
503 nanoparticle does not interfere in Dicer's ability to read and process siRNA sequences, but also
504 provided design principles of incorporation of Dicer-substrate siRNA onto the nanoparticles. It
505 can be concluded that the siRNA must be longer than 21 nt in length and allows for flexibility of
506 chemical modifications and the inclusion of phosphate and linker nucleotides, albeit at a slight
507 efficiency penalty. We have thus proven here, along with previous studies, RNA nanoparticles
508 serve as a powerful platform for the efficient delivery of siRNA.

509 **Acknowledgements**

511 The work was partially supported by NIH grants U01CA207946 and R01EB019036 to P.G
512 and the Cancer Prevention and Research Institute of Texas (CPRIT) [RP200615] and NIH grant
513 R03CA252770 to TJL. The content is solely the responsibility of the authors and does not
514 necessarily represent the official views of NIH. P.G.'s Sylvan G. Frank Endowed Chair position
515 in Pharmaceutics and Drug Delivery is funded by the CM Chen Foundation. Confocal images
516 presented in this report were generated using the instruments and services at the Campus
517 Microscopy and Imaging Facility, The Ohio State University. This facility is supported in part by
518 grant P30 CA016058, National Cancer Institute, Bethesda, MD.

519

520 Conflict of Interest

521 P.G. is the consultant of Oxford Nanopore Technologies; the cofounder of Shenzhen P&Z Bio-
522 medical Co. Ltd, as well as cofounder of ExonanoRNA, LLC and its subsidiary Weina
523 Biomedical LLC in Foshan. The content is solely the responsibility of the authors and does not
524 necessarily represent the official views of NIH.

525

526 Author Contributions

527 Conceptualization, P.G., S.G.; Methodology, S.G., H.Y., P.G., T.J.L.; Investigation, S.G.,
528 H.Y., T.J.L.; Writing-Original Draft, H.Y., D.W.B., P.G.; Writing-Review & Editing, D.W.B.,
529 S.L., P.G.; Visualization, D.W.B., S.G., P.G.; Funding Acquisition, P.G.

530

531 **Keywords:** RNA nanotechnology; dicer processing; gene regulation; siRNA delivery;
532 exosomes; nanobiotechnology; RNA therapeutics; RNA for cancer therapy

533

534 References

- 535 1. Agrawal, N, Dasaradhi, PV, Mohmmmed, A, Malhotra, P, Bhatnagar, RK, and Mukherjee,
536 SK (2003). RNA interference: biology, mechanism, and applications. *Microbiol Mol Biol*
537 *Rev* **67**: 657-685.
- 538 2. Bernstein, E, Caudy, AA, Hammond, SM, and Hannon, GJ (2001). Role for a bidentate
539 ribonuclease in the initiation step of RNA interference. *Nature* **409**: 363-366.

- 540 3. Lam, JK, Chow, MY, Zhang, Y, and Leung, SW (2015). siRNA Versus miRNA as
541 Therapeutics for Gene Silencing. *Mol Ther Nucleic Acids* **4**: e252.
- 542 4. Couzin, J (2002). Breakthrough of the year. Small RNAs make big splash. *Science* **298**:
543 2296-2297.
- 544 5. Fire, A, Xu, S, Montgomery, MK, Kostas, SA, Driver, SE, and Mello, CC (1998). Potent
545 and Specific Genetic Interference by Double-stranded RNA in *Caenorhabditis Elegans*.
546 *Nature* **391**: 806-811.
- 547 6. Elbashir, SM, Harborth, J, Lendeckel, W, Yalcin, A, Weber, K, and Tuschl, T (2001).
548 Duplexes of 21-nucleotide RNAs mediate RNA interference in cultured mammalian
549 cells. *Nature* **411**: 494-498.
- 550 7. Hoy, SM (2018). Patisiran: First Global Approval. *Drugs* **78**: 1625-1631.
- 551 8. Urits, I, Swanson, D, Swett, MC, Patel, A, Berardino, K, Amgalan, A, Berger, AA,
552 Kassem, H, Kaye, AD, and Viswanath, O (2020). A Review of Patisiran
553 (ONPATTRO(R)) for the Treatment of Polyneuropathy in People with Hereditary
554 Transthyretin Amyloidosis. *Neurol Ther* **9**: 301-315.
- 555 9. Goma-Garces, E, Perez-Gomez, MV, and Ortiz, A (2020). Givosiran for Acute
556 Intermittent Porphyria. *N Engl J Med* **383**: 1989.
- 557 10. Scott, LJ (2020). Givosiran: First Approval. *Drugs* **80**: 335-339.
- 558 11. Scott, LJ, and Keam, SJ (2021). Lumasiran: First Approval. *Drugs* **81**: 277-282.
- 559 12. Shu, Y, Pi, F, Sharma, A, Rajabi, M, Haque, F, Shu, D, Leggas, M, Evers, BM, and Guo,
560 P (2014). Stable RNA nanoparticles as potential new generation drugs for cancer therapy.
561 *Adv Drug Deliv Rev* **66**: 74-89.

- 562 13. Wang, HW, Noland, C, Siridechadilok, B, Taylor, DW, Ma, E, Felderer, K, Doudna, JA,
563 and Nogales, E (2009). Structural insights into RNA processing by the human RISC-
564 loading complex. *Nat Struct Mol Biol* **16**: 1148-1153.
- 565 14. Raja, MAG, Katas, H, and Amjad, MW (2019). Design, mechanism, delivery and
566 therapeutics of canonical and Dicer-substrate siRNA. *Asian J Pharm Sci* **14**: 497-510.
- 567 15. Gregory, RI, Chendrimada, TP, Cooch, N, and Shiekhattar, R (2005). Human RISC
568 couples microRNA biogenesis and posttranscriptional gene silencing. *Cell* **123**: 631-640.
- 569 16. Kim, DH, Behlke, MA, Rose, SD, Chang, MS, Choi, S, and Rossi, JJ (2005). Synthetic
570 dsRNA Dicer substrates enhance RNAi potency and efficacy. *Nat Biotechnol* **23**: 222-
571 226.
- 572 17. Hoerter, JA, and Walter, NG (2007). Chemical Modification Resolves the Asymmetry of
573 siRNA Strand Degradation in Human Blood Serum. *RNA* **13**: 1887-1893.
- 574 18. Watts, JK, Deleavey, GF, and Damha, MJ (2008). Chemically modified siRNA: tools and
575 applications. *Drug Discov Today* **13**: 842-855.
- 576 19. Bramsen, JB, and Kjems, J (2011). Chemical modification of small interfering RNA.
577 *Methods Mol Biol* **721**: 77-103.
- 578 20. Jackson, AL, Burchard, J, Leake, D, Reynolds, A, Schelter, J, Guo, J, Johnson, JM, Lim,
579 L, Karpilow, J, Nichols, K, *et al.* (2006). Position-specific Chemical Modification of
580 siRNAs Reduces "Off-target" Transcript Silencing. *RNA* **12**: 1197-1205.
- 581 21. Selvam, C, Mutisya, D, Prakash, S, Ranganna, K, and Thilagavathi, R (2017).
582 Therapeutic potential of chemically modified siRNA: Recent trends. *Chem Biol Drug*
583 *Des* **90**: 665-678.

- 584 22. Lau, PW, Guiley, KZ, De, N, Potter, CS, Carragher, B, and MacRae, IJ (2012). The
585 molecular architecture of human Dicer. *Nat Struct Mol Biol* **19**: 436-440.
- 586 23. Sashital, DG, and Doudna, JA (2010). Structural insights into RNA interference. *Curr*
587 *Opin Struct Biol* **20**: 90-97.
- 588 24. Song, JJ, Liu, J, Tolia, NH, Schneiderman, J, Smith, SK, Martienssen, RA, Hannon, GJ,
589 and Joshua-Tor, L (2003). The crystal structure of the Argonaute2 PAZ domain reveals
590 an RNA binding motif in RNAi effector complexes. *Nat Struct Biol* **10**: 1026-1032.
- 591 25. Podolska, K, Sedlak, D, Bartunek, P, and Svoboda, P (2014). Fluorescence-based high-
592 throughput screening of dicer cleavage activity. *J Biomol Screen* **19**: 417-426.
- 593 26. Harborth, J, Elbashir, SM, Vandeburgh, K, Manninga, H, Scaringe, SA, Weber, K, and
594 Tuschl, T (2003). Sequence, chemical, and structural variation of small interfering RNAs
595 and short hairpin RNAs and the effect on mammalian gene silencing. *Antisense Nucleic*
596 *Acid Drug Dev* **13**: 83-105.
- 597 27. MacRae, IJ, Zhou, K, and Doudna, JA (2007). Structural determinants of RNA
598 recognition and cleavage by Dicer. *Nat Struct Mol Biol* **14**: 934-940.
- 599 28. Park, JE, Heo, I, Tian, Y, Simanshu, DK, Chang, H, Jee, D, Patel, DJ, and Kim, VN
600 (2011). Dicer recognizes the 5' end of RNA for efficient and accurate processing. *Nature*
601 **475**: 201-205.
- 602 29. Vermeulen, A, Behlen, L, Reynolds, A, Wolfson, A, Marshall, WS, Karpilow, J, and
603 Khvorova, A (2005). The contributions of dsRNA structure to Dicer specificity and
604 efficiency. *RNA* **11**: 674-682.

- 605 30. Pi, F, Binzel, DW, Lee, TJ, Li, Z, Sun, M, Rychahou, P, Li, H, Haque, F, Wang, S,
606 Croce, CM, *et al.* (2018). Nanoparticle orientation to control RNA loading and ligand
607 display on extracellular vesicles for cancer regression. *Nat Nanotechnol* **13**: 82-89.
- 608 31. Guo, P, Coban, O, Snead, NM, Trebley, J, Hoeplich, S, Guo, S, and Shu, Y (2010).
609 Engineering RNA for targeted siRNA delivery and medical application. *Adv Drug Deliv*
610 *Rev* **62**: 650-666.
- 611 32. Jasinski, D, Haque, F, Binzel, DW, and Guo, P (2017). Advancement of the Emerging
612 Field of RNA Nanotechnology. *ACS Nano* **11**: 1142-1164.
- 613 33. Xu, C, Haque, F, Jasinski, DL, Binzel, DW, Shu, D, and Guo, P (2018). Favorable
614 biodistribution, specific targeting and conditional endosomal escape of RNA
615 nanoparticles in cancer therapy. *Cancer Lett* **414**: 57-70.
- 616 34. Guo, P (2010). The emerging field of RNA nanotechnology. *Nat Nanotechnol* **5**: 833-
617 842.
- 618 35. Guo, P, Zhang, C, Chen, C, Garver, K, and Trottier, M (1998). Inter-RNA interaction of
619 phage phi29 pRNA to form a hexameric complex for viral DNA transportation. *Mol Cell*
620 **2**: 149-155.
- 621 36. Shu, D, Shu, Y, Haque, F, Abdelmawla, S, and Guo, P (2011). Thermodynamically stable
622 RNA three-way junction for constructing multifunctional nanoparticles for delivery of
623 therapeutics. *Nat Nanotechnol* **6**: 658-667.
- 624 37. Khisamutdinov, EF, Jasinski, DL, and Guo, P (2014). RNA as a Boiling-Resistant
625 Anionic Polymer Material to Build Robust Structures with Defined Shape and
626 Stoichiometry. *ACS Nano* **8**: 4771-4781.

- 627 38. Piao, X, Wang, H, Binzel, DW, and Guo, P (2018). Assessment and Comparison of
628 Thermal Stability of Phosphorothioate-DNA, DNA, RNA, 2'-F RNA, and LNA in the
629 Context of Phi29 pRNA 3WJ. *RNA* **24**: 67-76.
- 630 39. Haque, F, Shu, D, Shu, Y, Shlyakhtenko, LS, Rychahou, PG, Evers, BM, and Guo, P
631 (2012). Ultrastable Synergistic Tetravalent RNA Nanoparticles for Targeting to Cancers.
632 *Nano Today* **7**: 245-257.
- 633 40. Shu, Y, Haque, F, Shu, D, Li, W, Zhu, Z, Kotb, M, Lyubchenko, Y, and Guo, P (2013).
634 Fabrication of 14 Different RNA Nanoparticles for Specific Tumor Targeting Without
635 Accumulation in Normal Organs. *RNA* **19**: 767-777.
- 636 41. Liu, J, Guo, S, Cinier, M, Shlyakhtenko, LS, Shu, Y, Chen, C, Shen, G, and Guo, P
637 (2011). Fabrication of Stable and RNase-resistant RNA Nanoparticles Active in Gearing
638 the Nanomotors for Viral DNA Packaging. *ACS Nano* **5**: 237-246.
- 639 42. Abdelmawla, S, Guo, S, Zhang, L, Pulukuri, SM, Patankar, P, Conley, P, Trebley, J, Guo,
640 P, and Li, QX (2011). Pharmacological Characterization of Chemically Synthesized
641 Monomeric Phi29 pRNA Nanoparticles for Systemic Delivery. *Mol Ther* **19**: 1312-1322.
- 642 43. Shu, D, Khisamutdinov, EF, Zhang, L, and Guo, P (2014). Programmable folding of
643 fusion RNA in vivo and in vitro driven by pRNA 3WJ motif of phi29 DNA packaging
644 motor. *Nucleic Acids Res* **42**: e10.
- 645 44. Cui, D, Zhang, C, Liu, B, Shu, Y, Du, T, Shu, D, Wang, K, Dai, F, Liu, Y, Li, C, *et al.*
646 (2015). Regression of Gastric Cancer by Systemic Injection of RNA Nanoparticles
647 Carrying both Ligand and siRNA. *Sci Rep* **5**: 10726.
- 648 45. Rychahou, P, Haque, F, Shu, Y, Zaytseva, Y, Weiss, HL, Lee, EY, Mustain, W,
649 Valentino, J, Guo, P, and Evers, BM (2015). Delivery of RNA Nanoparticles into

- 650 Colorectal Cancer Metastases Following Systemic Administration. *ACS Nano* **9**: 1108-
651 1116.
- 652 46. Lee, TJ, Haque, F, Shu, D, Yoo, JY, Li, H, Yokel, RA, Horbinski, C, Kim, TH, Kim, SH,
653 Kwon, CH, *et al.* (2015). RNA Nanoparticle as a Vector for Targeted siRNA Delivery
654 into Glioblastoma Mouse Model. *Oncotarget* **6**: 14766-14776.
- 655 47. S, ELA, Mager, I, Breakefield, XO, and Wood, MJ (2013). Extracellular vesicles:
656 biology and emerging therapeutic opportunities. *Nat Rev Drug Discov* **12**: 347-357.
- 657 48. Valadi, H, Ekstrom, K, Bossios, A, Sjostrand, M, Lee, JJ, and Lotvall, JO (2007).
658 Exosome-mediated transfer of mRNAs and microRNAs is a novel mechanism of genetic
659 exchange between cells. *Nat Cell Biol* **9**: 654-659.
- 660 49. Alvarez-Erviti, L, Seow, Y, Yin, H, Betts, C, Lakhali, S, and Wood, MJ (2011). Delivery
661 of siRNA to the mouse brain by systemic injection of targeted exosomes. *Nat Biotechnol*
662 **29**: 341-345.
- 663 50. Ohno, S, Takanashi, M, Sudo, K, Ueda, S, Ishikawa, A, Matsuyama, N, Fujita, K,
664 Mizutani, T, Ohgi, T, Ochiya, T, *et al.* (2013). Systemically injected exosomes targeted
665 to EGFR deliver antitumor microRNA to breast cancer cells. *Mol Ther* **21**: 185-191.
- 666 51. Shtam, TA, Kovalev, RA, Varfolomeeva, EY, Makarov, EM, Kil, YV, and Filatov, MV
667 (2013). Exosomes are natural carriers of exogenous siRNA to human cells in vitro. *Cell*
668 *Commun Signal* **11**: 88.
- 669 52. van Dommelen, SM, Vader, P, Lakhali, S, Kooijmans, SA, van Solinge, WW, Wood, MJ,
670 and Schiffelers, RM (2012). Microvesicles and exosomes: opportunities for cell-derived
671 membrane vesicles in drug delivery. *J Control Release* **161**: 635-644.

- 672 53. Al-Nedawi, K, Meehan, B, Micallef, J, Lhotak, V, May, L, Guha, A, and Rak, J (2008).
673 Intercellular transfer of the oncogenic receptor EGFRvIII by microvesicles derived from
674 tumour cells. *Nat Cell Biol* **10**: 619-624.
- 675 54. Skog, J, Wurdinger, T, van Rijn, S, Meijer, DH, Gainche, L, Sena-Esteves, M, Curry,
676 WT, Jr., Carter, BS, Krichevsky, AM, and Breakefield, XO (2008). Glioblastoma
677 microvesicles transport RNA and proteins that promote tumour growth and provide
678 diagnostic biomarkers. *Nat Cell Biol* **10**: 1470-1476.
- 679 55. El Andaloussi, S, Lakhali, S, Mager, I, and Wood, MJ (2013). Exosomes for targeted
680 siRNA delivery across biological barriers. *Adv Drug Deliv Rev* **65**: 391-397.
- 681 56. Zheng, Z, Li, Z, Xu, C, Guo, B, and Guo, P (2019). Folate-displaying exosome mediated
682 cytosolic delivery of siRNA avoiding endosome trapping. *J Control Release* **311-312**: 43-
683 49.
- 684 57. Afonin, KA, Cieply, DJ, and Leontis, NB (2008). Specific RNA self-assembly with
685 minimal paranemic motifs. *J Am Chem Soc* **130**: 93-102.
- 686 58. Chworos, A, Severcan, I, Koyfman, AY, Weinkam, P, Oroudjev, E, Hansma, HG, and
687 Jaeger, L (2004). Building Programmable Jigsaw Puzzles with RNA. *Science* **306**: 2068-
688 2072.
- 689 59. Geary, C, Rothmund, PW, and Andersen, ES (2014). RNA Nanostructures. A Single-
690 stranded Architecture for Cotranscriptional Folding of RNA Nanostructures. *Science* **345**:
691 799-804.
- 692 60. Grabow, WW, and Jaeger, L (2014). RNA self-assembly and RNA nanotechnology. *Acc*
693 *Chem Res* **47**: 1871-1880.

- 694 61. Hansma, HG, Oroudjev, E, Baudrey, S, and Jaeger, L (2003). TectoRNA and 'kissing-
695 loop' RNA: atomic force microscopy of self-assembling RNA structures. *J Microsc* **212**:
696 273-279.
- 697 62. Hao, C, Li, X, Tian, C, Jiang, W, Wang, G, and Mao, C (2014). Construction of RNA
698 nanocages by re-engineering the packaging RNA of Phi29 bacteriophage. *Nat Commun*
699 **5**: 3890.
- 700 63. Jaeger, L, Westhof, E, and Leontis, NB (2001). TectoRNA: modular assembly units for
701 the construction of RNA nano-objects. *Nucleic Acids Res* **29**: 455-463.
- 702 64. Ohno, H, and Saito, H (2016). RNA and RNP as Building Blocks for Nanotechnology
703 and Synthetic Biology. *Prog Mol Biol Transl Sci* **139**: 165-185.
- 704 65. Jedrzejczyk, D, and Chworos, A (2019). Self-Assembling RNA Nanoparticle for Gene
705 Expression Regulation in a Model System. *ACS Synth Biol* **8**: 491-497.
- 706 66. Afonin, KA, Kireeva, M, Grabow, WW, Kashlev, M, Jaeger, L, and Shapiro, BA (2012).
707 Co-transcriptional assembly of chemically modified RNA nanoparticles functionalized
708 with siRNAs. *Nano Lett* **12**: 5192-5195.
- 709 67. Stewart, JM, Viard, M, Subramanian, HK, Roark, BK, Afonin, KA, and Franco, E
710 (2016). Programmable RNA Microstructures for Coordinated Delivery of siRNAs.
711 *Nanoscale* **8**: 17542-17550.
- 712 68. Zakrevsky, P, Kasprzak, WK, Heinz, WF, Wu, W, Khant, H, Bindewald, E, Dorjsuren,
713 N, Fields, EA, de Val, N, Jaeger, L, *et al.* (2020). Truncated Tetrahedral RNA
714 Nanostructures Exhibit Enhanced Features for Delivery of RNAi Substrates. *Nanoscale*
715 **12**: 2555-2568.

- 716 69. Rackley, L, Stewart, JM, Salotti, J, Krokhotin, A, Shah, A, Halman, JR, Juneja, R,
717 Smollett, J, Lee, L, Roark, K, *et al.* (2018). RNA Fibers as Optimized Nanoscaffolds for
718 siRNA Coordination and Reduced Immunological Recognition. *Adv Funct Mater* **28**:
719 1805959.
- 720 70. Lee, JB, Hong, J, Bonner, DK, Poon, Z, and Hammond, PT (2012). Self-assembled RNA
721 interference microsponges for efficient siRNA delivery. *Nat Mater* **11**: 316-322.
- 722 71. Halman, JR, Kim, KT, Gwak, SJ, Pace, R, Johnson, MB, Chandler, MR, Rackley, L,
723 Viard, M, Marriott, I, Lee, JS, *et al.* (2020). A Cationic Amphiphilic Co-polymer as a
724 Carrier of Nucleic Acid Nanoparticles (Nanps) for Controlled Gene Silencing,
725 Immunostimulation, and Biodistribution. *Nanomedicine* **23**: 102094-102106.
- 726 72. Nordmeier, S, Ke, W, Afonin, KA, and Portnoy, V (2020). Exosome Mediated Delivery
727 of Functional Nucleic Acid Nanoparticles (NANPs). *Nanomedicine* **30**: 102285-102296.
- 728 73. Frohman, MA, Dush, MK, and Martin, GR (1988). Rapid production of full-length
729 cDNAs from rare transcripts: amplification using a single gene-specific oligonucleotide
730 primer. *Proc Natl Acad Sci U S A* **85**: 8998-9002.
- 731 74. Zhang, HM, Su, Y, Guo, S, Yuan, J, Lim, T, Liu, J, Guo, P, and Yang, D (2009).
732 Targeted delivery of anti-coxsackievirus siRNAs using ligand-conjugated packaging
733 RNAs. *Antiviral Res* **83**: 307-316.
- 734 75. Binzel, DW, Shu, Y, Li, H, Sun, M, Zhang, Q, Shu, D, Guo, B, and Guo, P (2016).
735 Specific Delivery of MiRNA for High Efficient Inhibition of Prostate Cancer by RNA
736 Nanotechnology. *Mol Ther* **24**: 1267-1277.
- 737 76. Binzel, DW, Khisamutdinov, EF, and Guo, P (2014). Entropy-driven One-step Formation
738 of Phi29 pRNA 3WJ from Three RNA Fragments. *Biochemistry* **53**: 2221-2231.

- 739 77. Harding, C, and Stahl, P (1983). Transferrin recycling in reticulocytes: pH and iron are
740 important determinants of ligand binding and processing. *Biochem Biophys Res Commun*
741 **113**: 650-658.
- 742 78. Li, Z, Wang, H, Yin, H, Bennett, C, Zhang, HG, and Guo, P (2018). Arrowtail RNA for
743 Ligand Display on Ginger Exosome-like Nanovesicles to Systemic Deliver siRNA for
744 Cancer Suppression. *Sci Rep* **8**: 14644.
- 745 79. Pi, F, Binzel, DW, Lee, TJ, Li, Z, Sun, M, Rychahou, P, Li, H, Haque, F, Wang, S,
746 Croce, CM, *et al.* (2018). Nanoparticle Orientation to Control RNA Loading and Ligand
747 Display on Extracellular Vesicles for Cancer Regression. *Nat Nanotechnol* **13**: 82-89.
- 748 80. Gu, S, Jin, L, Zhang, Y, Huang, Y, Zhang, F, Valdmanis, PN, and Kay, MA (2012). The
749 loop position of shRNAs and pre-miRNAs is critical for the accuracy of dicer processing
750 in vivo. *Cell* **151**: 900-911.
- 751 81. Lau, PW, Potter, CS, Carragher, B, and MacRae, IJ (2009). Structure of the human Dicer-
752 TRBP complex by electron microscopy. *Structure* **17**: 1326-1332.
- 753 82. Li, Z, Yang, L, Wang, H, Binzel, DW, Williams, TM, and Guo, P (2021). Non-Small-
754 Cell Lung Cancer Regression by siRNA Delivered Through Exosomes That Display
755 EGFR RNA Aptamer. *Nucleic Acid Ther*: 10.1089/nat.2021.0002.
- 756 83. Charbe, NB, Amnerkar, ND, Ramesh, B, Tambuwala, MM, Bakshi, HA, Aljabali, AAA,
757 Khadse, SC, Satheeshkumar, R, Satija, S, Metha, M, *et al.* (2020). Small interfering RNA
758 for cancer treatment: overcoming hurdles in delivery. *Acta Pharm Sin B* **10**: 2075-2109.
- 759 84. (2006). A billion dollar punt. *Nat Biotechnol* **24**: 1453.
- 760 85. Duchaine, TF, and Slack, FJ (2009). RNA interference and micro RNA-oriented therapy
761 in cancer: rationales, promises, and challenges. *Curr Oncol* **16**: 61-66.

- 762 86. Couzin-Frankel, J (2010). Drug research. Roche exits RNAi field, cuts 4800 jobs. *Science*
763 **330**: 1163.
- 764 87. Huggett, B, and Paisner, K (2017). The commercial tipping point. *Nat Biotechnol* **35**:
765 708-709.
- 766 88. Haussecker, D (2008). The business of RNAi therapeutics. *Hum Gene Ther* **19**: 451-462.
- 767 89. Morrison, C (2018). Alnylam prepares to land first RNAi drug approval. *Nat Rev Drug*
768 *Discov* **17**: 156-157.
- 769 90. Collingwood, MA, Rose, SD, Huang, L, Hillier, C, Amarzguioui, M, Wiüger, MT, Soifer,
770 HS, Rossi, JJ, and Behlke, MA (2008). Chemical modification patterns compatible with
771 high potency dicer-substrate small interfering RNAs. *Oligonucleotides* **18**: 187-200.
- 772 91. Foster, DJ, Barros, S, Duncan, R, Shaikh, S, Cantley, W, Dell, A, Bulgakova, E, O'Shea,
773 J, Taneja, N, Kuchimanchi, S, *et al.* (2012). Comprehensive evaluation of canonical
774 versus Dicer-substrate siRNA in vitro and in vivo. *RNA* **18**: 557-568.
- 775 92. Salomon, W, Bullock, K, Lapierre, J, Pavco, P, Woolf, T, and Kamens, J (2010).
776 Modified dsRNAs that are not processed by Dicer maintain potency and are incorporated
777 into the RISC. *Nucleic Acids Res* **38**: 3771-3779.
- 778 93. Ghimire, C, Wang, H, Li, H, Vieweger, M, Xu, C, and Guo, P (2020). RNA
779 Nanoparticles as Rubber for Compelling Vessel Extravasation to Enhance Tumor
780 Targeting and for Fast Renal Excretion to Reduce Toxicity. *ACS Nano* **14**: 13180-13191.
- 781 94. Saw, PE, and Song, EW (2020). siRNA therapeutics: a clinical reality. *Sci China Life Sci*
782 **63**: 485-500.
- 783 95. Yonezawa, S, Koide, H, and Asai, T (2020). Recent advances in siRNA delivery
784 mediated by lipid-based nanoparticles. *Adv Drug Deliv Rev* **154-155**: 64-78.

- 785 96. Lin, Q, Chen, J, Zhang, Z, and Zheng, G (2014). Lipid-based nanoparticles in the
786 systemic delivery of siRNA. *Nanomedicine (Lond)* **9**: 105-120.
- 787 97. Li, T, Huang, L, and Yang, M (2020). Lipid-based Vehicles for siRNA Delivery in
788 Biomedical Field. *Curr Pharm Biotechnol* **21**: 3-22.
- 789 98. Nair, JK, Attarwala, H, Sehgal, A, Wang, Q, Aluri, K, Zhang, X, Gao, M, Liu, J,
790 Indrakanti, R, Schofield, S, *et al.* (2017). Impact of enhanced metabolic stability on
791 pharmacokinetics and pharmacodynamics of GalNAc-siRNA conjugates. *Nucleic Acids*
792 *Res* **45**: 10969-10977.
- 793 99. Foster, DJ, Brown, CR, Shaikh, S, Trapp, C, Schlegel, MK, Qian, K, Sehgal, A, Rajeev,
794 KG, Jadhav, V, Manoharan, M, *et al.* (2018). Advanced siRNA Designs Further Improve
795 In Vivo Performance of GalNAc-siRNA Conjugates. *Mol Ther* **26**: 708-717.
- 796 100. Springer, AD, and Dowdy, SF (2018). GalNAc-siRNA Conjugates: Leading the Way for
797 Delivery of RNAi Therapeutics. *Nucleic Acid Ther* **28**: 109-118.
- 798 101. Turner, AM, Stolk, J, Bals, R, Lickliter, JD, Hamilton, J, Christianson, DR, Given, BD,
799 Burdon, JG, Loomba, R, Stoller, JK, *et al.* (2018). Hepatic-targeted RNA interference
800 provides robust and persistent knockdown of alpha-1 antitrypsin levels in ZZ patients. *J*
801 *Hepatol* **69**: 378-384.
- 802 102. Sebestyen, MG, Wong, SC, Trubetskoy, V, Lewis, DL, and Wooddell, CI (2015).
803 Targeted in vivo delivery of siRNA and an endosome-releasing agent to hepatocytes.
804 *Methods Mol Biol* **1218**: 163-186.
- 805 103. Guo, S, Vieweger, M, Zhang, K, Yin, H, Wang, H, Li, X, Li, S, Hu, S, Sparreboom, A,
806 Evers, BM, *et al.* (2020). Ultra-thermostable RNA nanoparticles for solubilizing and
807 high-yield loading of paclitaxel for breast cancer therapy. *Nat Commun* **11**: 972.

- 808 104. Shu, D, Li, H, Shu, Y, Xiong, G, Carson, WE, 3rd, Haque, F, Xu, R, and Guo, P (2015).
809 Systemic Delivery of Anti-miRNA for Suppression of Triple Negative Breast Cancer
810 Utilizing RNA Nanotechnology. *ACS Nano* **9**: 9731-9740.
- 811 105. Wang, H, Ellipilli, S, Lee, WJ, Li, X, Vieweger, M, Ho, YS, and Guo, P (2021).
812 Multivalent rubber-like RNA nanoparticles for targeted co-delivery of paclitaxel and
813 MiRNA to silence the drug efflux transporter and liver cancer drug resistance. *J Control*
814 *Release* **330**: 173-184.
- 815 106. Zhang, Y, Leonard, M, Shu, Y, Yang, Y, Shu, D, Guo, P, and Zhang, X (2017).
816 Overcoming Tamoxifen Resistance of Human Breast Cancer by Targeted Gene Silencing
817 Using Multifunctional pRNA Nanoparticles. *ACS Nano* **11**: 335-346.
- 818 107. Xu, Y, Pang, L, Wang, H, Xu, C, Shah, H, Guo, P, Shu, D, and Qian, SY (2019). Specific
819 delivery of delta-5-desaturase siRNA via RNA nanoparticles supplemented with dihomom-
820 gamma-linolenic acid for colon cancer suppression. *Redox Biol* **21**: 101085.
- 821 108. Shu, Y, Shu, D, Haque, F, and Guo, P (2013). Fabrication of pRNA nanoparticles to
822 deliver therapeutic RNAs and bioactive compounds into tumor cells. *Nat Protoc* **8**: 1635-
823 1659.
- 824

825 List of Figure Legends

826
827 **Figure 1: Identification of the specific cleavage site of mRNA delivered by RNA**
828 **nanoparticles into KB cells. A.** Site specific cleavage of Lamin A/C mRNA induced by pRNA-
829 lamin demonstrated by 5' RACE. pRNA-lamin25 was constructed by linking a siRNA sequence
830 (underlined) with a pRNA vector via UU linkers at the sense (upper) and antisense (lower)
831 strand. Sequences of Lamin A/C mRNA that are identical with the siRNA were underlined, and
832 the cleavage site was marked with a star. Sequencing results shows that the PCR product
833 contains a RNA ligator sequence (red) and part of the Lamin A/C mRNA sequence. **B.** PCR
834 products resulting from outer primer pairs were separated in 1.2% agarose gel.

835
836 **Figure 2: Construction and stability studies of 3WJ/Luc2-siRNA. A.** Design of 3WJ/*LUC2*-
837 siRNA molecular beacon (Red star: Cy5 fluorophore, Black circle: BBQ650 quencher). **B.**
838 Assembly of 3WJ/*LUC2*-siRNA molecular beacon assayed by 15% Native PAGE (green: EtBr,
839 Red: Cy5, Yellow: overlap). **C.** Serum stability and **D.** thermodynamic stability of 3WJ/*LUC2*-
840 siRNA assayed by 15% Native PAGE.

841
842 **Figure 3: Experimental design for intracellular imaging studies. A.** Folate-Exosomes designs
843 carrying RNA nanoparticle beacons (3WJ/*LUC2*-siRNA-truncated beacon, 3WJ/*LUC2*-siRNA
844 beacon, 3WJ/*LUC2*-siRNA/Cy5); Red star: Cy5 fluorophore, Black circle: BBQ650 quencher. **B.**
845 Intracellular imaging of Dicer processing of 3WJ/*LUC2*-siRNA delivered by exosomes after 0.5
846 hr incubation with HT29 cells. **C.** Intracellular imaging of Dicer processing of 3WJ/*LUC2*-
847 siRNA delivered by exosomes after 2 hr incubation with HT29 cells. **D.** Intracellular imaging of

848 Dicer processing of 3WJ/*LUC2*-siRNA delivered by exosomes after 4 hr incubation with HT29
849 cells. Blue: nuclei, Green: Cytoskeleton, Red: RNA.

850

851 **Figure 4: The impact of siRNA length and chemical modifications on Dicer processing. A.**

852 *In vitro* Dicer processing of DS/*LUC2*-siRNA in different length. (19-, 21-, 22-, 23-, 24- bp; p:

853 phosphate group; S: sense strand; AS: antisense strand). **B.** and **C.** *In vitro* Dicer processing of

854 different designs of DS/*LUC2*-siRNA. (p: phosphate group; S: sense strand; AS: antisense

855 strand). Each sample was run as siRNA control without Dicer (-) and with Dicer (+). **D.** *In vitro*

856 processing of siRNA from 3WJ RNA nanoparticles when incubated with cell lysates. In **A-C**, the

857 treated siRNAs were separated in 1.2% agarose gels; and in **D**, separated in 15% Native PAGE.

858 All siRNA cleavage was calculated by gel band quantified by Image J.

859

860 **Figure 5: Summary of previous animal trials to elucidate the processing and releasing of**

861 **Survivin siRNA incorporated in the RNA nanoparticles, as shown in models of non-small-**

862 **cell lung,⁸² breast,³⁰ prostate cancer.³⁰** RNA nanoparticles harboring Survivin siRNA were

863 loaded into exosomes and decorated with either EGFR (epidermal growth factor) or PSMA

864 (prostate specific membrane antigen) RNA aptamers and delivered to prostate cancer, triple

865 negative breast cancer (TNBC), and non-small-cell lung cancer (NSCLC) tumors in mice.

866 Repeated administration demonstrated strong tumor inhibition over control nanoparticles. The

867 data in this figure is the summary of previously published work. Inclusion of the previously

868 published animal data follows the journal policy of *Molecular Therapy Nucleic Acids*, with

869 figure copyright permission from the publishers and original data from the authors Ref^{30, 82}.

eTOC Synopsis

SiRNA for silencing genes and treating diseases has been a popular dream but not fully realized. Peixuan Guo and colleagues report the rational design of siRNA to RNA nanoparticles for efficient delivery while avoiding endosomes. Thus providing guidelines for siRNA design on RNA nanoparticles to overcome previous roadblocks.

Journal Pre-proof

A.

Sequence of pRNA-Lamin25

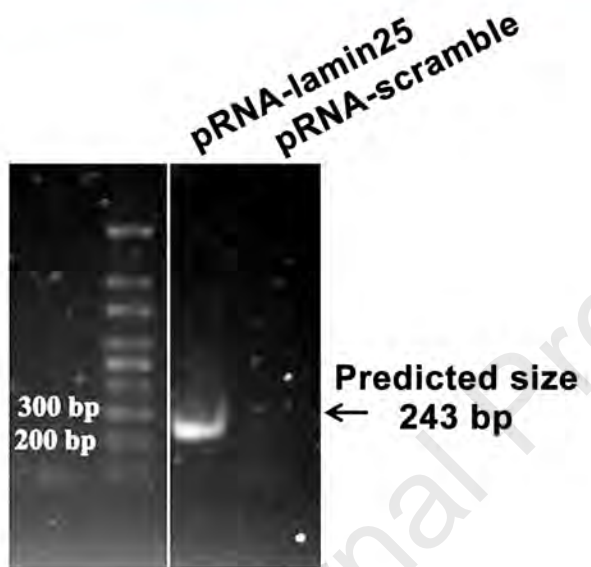
5'-cuGGAcuuccAGAAGAAcAucuAcA-uu-(pRNA vector)-3'

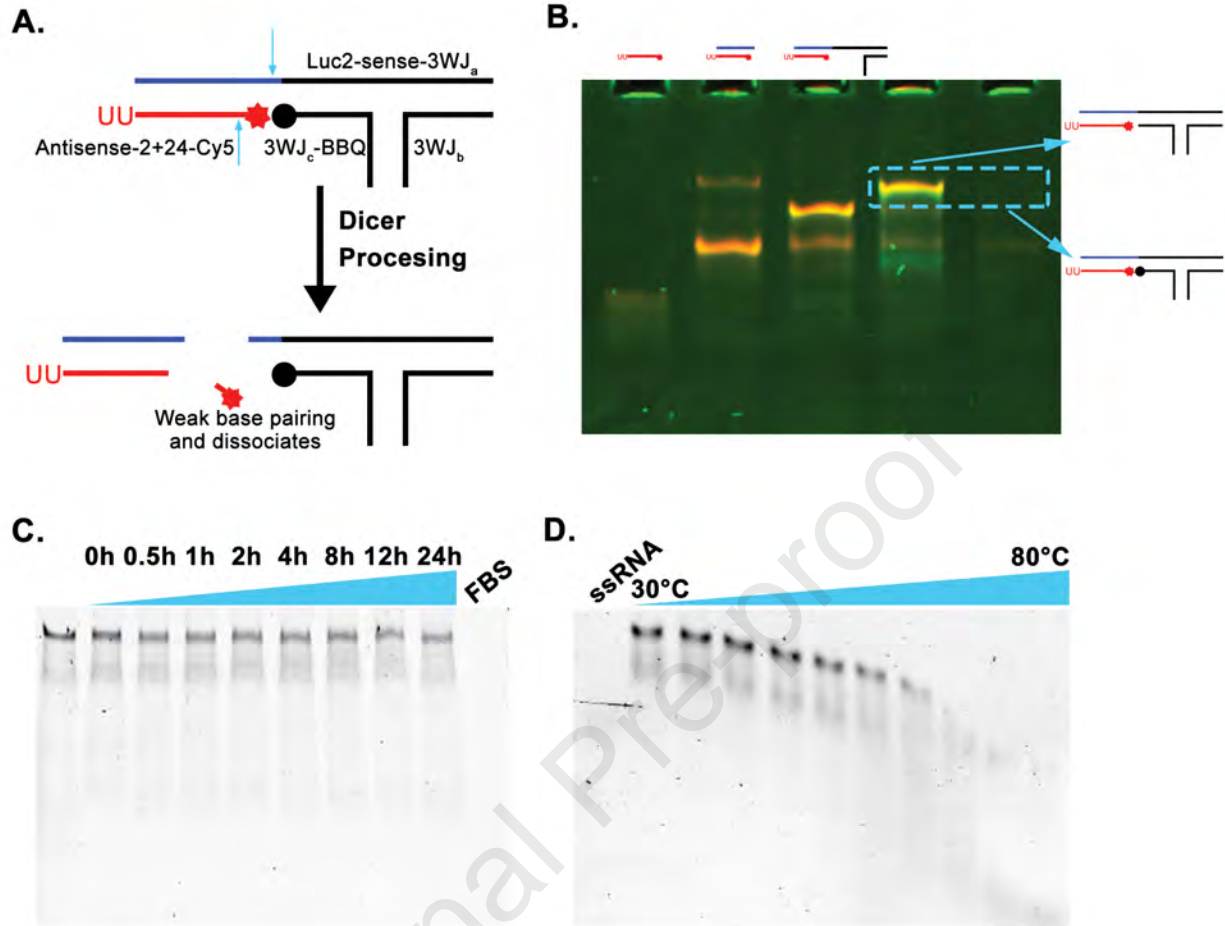
3'-uu-GAccuGAAGGucuucuuGuAGAuGu-uu-(pRNA vector)-5'

mRNA sequence of lamin gene5'...cagaccaugaaggaggaacuggacuuccagaag*aacaucuacagugag...-3'**Sequence of PCR product**5'-**NTCGCGGATCCGGAACACTGCGTTTGCTGGCTTTGATGAAA****AACATCTACAGTGAGGAGCTG**...-3'

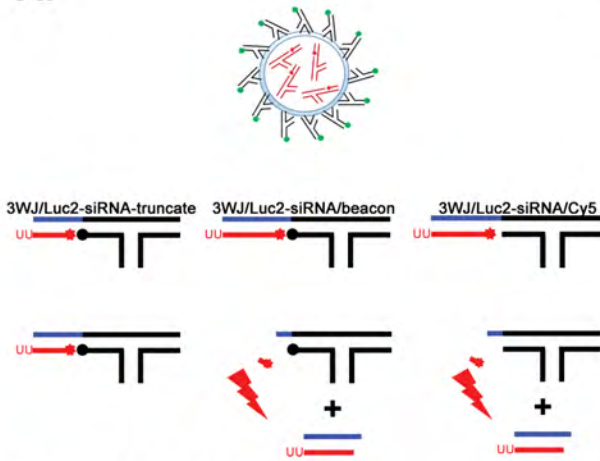
(-----RNA adaptor introduced by ligation-----)(-----mRNA sequence of lamin-----)

B.

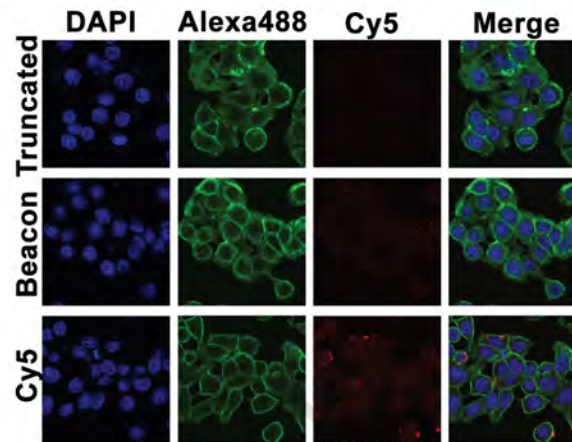




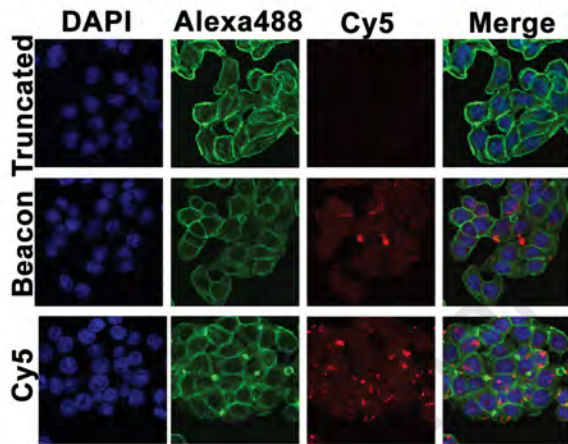
A.



B. 0.5 Hours



C. 2.0 Hours



D. 4.0 Hours

